0026-895X/06/7004-1319–1329$20.00
MOLECULAR PHARMACOLOGY
Copyright © 2006 The American Society for Pharmacology and Experimental Therapeutics
Mol Pharmacol 70:1319–1329, 2006

Vol. 70, No. 4
26492/3139347
Printed in U.S.A.

Biophysical Characterization of the New Human Ether-A-Go-Go-Related Gene Channel Opener NS3623 [*N*-(4-Bromo-2-(1*H*-tetrazol-5-yl)-phenyl)-*N*′-(3′-trifluoromethylphenyl)urea]

Rie Schultz Hansen, Thomas Goldin Diness, Torsten Christ, Erich Wettwer, Ursula Ravens, Søren-Peter Olesen, and Morten Grunnet

NeuroSearch A/S, Ballerup, Denmark (R.S.H., T.G.D., S.-P.O., M.G.); Danish National Research Foundation Centre for Cardiac Arrhythmia, University of Copenhagen, Copenhagen, Denmark (R.S.H., T.G.D., S.-P.O., M.G.); and Department of Pharmacology and Toxicology, Medical Faculty, Dresden University of Technology, Dresden, Germany (T.C., E.W., U.R.)

Received May 16, 2006; accepted July 5, 2006

ABSTRACT

Within the field of new antiarrhythmic compounds, the interesting idea of activating human ether-a-go-go-related gene (HERG1) potassium channels has recently been introduced. Potentially, drugs that increase HERG1 channel activity will augment the repolarizing current of the cardiac myocytes and stabilize the diastolic interval. This may make the myocardium more resistant to events that cause arrhythmias. We here present the compound *N*-(4-bromo-2-(1*H*-tetrazol-5-yl)-phenyl)-*N*′-(3′-trifluoromethylphenyl)urea (NS3623), which has the ability to activate HERG1 channels expressed in *Xenopus laevis* oocytes with an EC_{50} value of 79.4 μM. Exposure of HERG1 channels to NS3623 affects the voltage-dependent release from inactivation, resulting in a half-inactivation voltage that is rightward-shifted by 17.7 mV. Moreover, the compound affects the time constant of inactivation, leading to a slower onset of inactivation of the macroscopic HERG1 currents. We also characterized the ability of NS3623 to increase the activity of different mutated HERG1 channels. The mutants S620T and S631A are severely compromised in their ability to inactivate. Application of NS3623 to any of these two mutants did not result in increased HERG1 current. In contrast, application of NS3623 to the mutant F656M increased HERG1 current to a larger extent than what was observed with wild-type HERG1 channels. Because the amino acid F656 is essential for high-affinity inhibition of HERG1 channels, it is concluded that NS3623 has a dual mode of action, being both an activator and an inhibitor of HERG1 channels. Finally, we show that NS3623 has the ability to shorten action potential durations in guinea pig papillary muscle.

Potassium channels are essential for repolarizing the membrane potential of excitable cells and for maintaining the resting membrane potential between action potentials. In the heart, the delayed inward rectifying repolarizing potassium current I_K is composed of two currents, denoted I_{Kr} and I_{Ks}. Activation of the human ether-a-go-go-related gene (HERG1) potassium channels underlies the I_{Kr} (Sanguinetti et al., 1995; Trudeau et al., 1995), whereas the molecular component behind I_{Ks} is KCNQ1 potassium channels in association with KCNE1 β-subunits (Barhanin et al., 1996; Sanguinetti et al., 1996). The HERG1 channel has an architecture like many other voltage-gated potassium channels with homologous subunits containing six transmembrane domains that form a tetrameric channel. In addition, the HERG1 channel is recognized by its characteristic inward rectification properties. The inward rectification is caused by the unique ability of the HERG1 channel to slowly activate at depolarized membrane potentials followed by much faster C-type inactivation where the channel keeps a nonconducting configuration (Spector et al., 1996). When the membrane repolarizes, the channel is quickly released from inactivation and conducts a slowly deactivating current. The pore region of the HERG1 channel has aromatic residues at positions 652

This work was supported by the Danish National Research Foundation Center for Cardiac Arrhythmia.
Article, publication date, and citation information can be found at http://molpharm.aspetjournals.org.
doi:10.1124/mol.106.026492.

ABBREVIATIONS: HERG, human ether-a-go-go-related gene; APD, action potential duration; NS1643, 1,3-bis-(2-hydroxy-5-trifluoromethylphenyl)-urea; NS3623, *N*-(4-bromo-2-(1*H*-tetrazol-5-yl)-phenyl)-*N*′-(3′-trifluoromethylphenyl)urea; HEK, human embryonic kidney.

and 656, which point toward the central cavity, thereby rendering the channel rather promiscuous with respect to lipophilic drugs that can bind in the pore region, as well as blocking channel conduction (Mitcheson et al., 2005). Although blocking I_{Kr} has been a strategy for prevention of ventricular and more recently also atrial fibrillation, it is now known that this approach in some patients is likely to be proarrhythmic. Inhibiting HERG1 channel function prolongs cardiac action potential duration, and under certain conditions this may lead to lethal ventricular arrhythmias mediated by transient torsade de pointes (reviewed by Fitzgerald and Ackerman, 2005). Recently, a series of new molecules that activate the HERG1 channel has been discovered (Kang et al., 2005; Zhou et al., 2005; Hansen et al., 2006). The compounds all were effective in increasing the repolarizing reserve in cardiac myocytes, thereby significantly shortening the action potential duration (APD). Moreover, in one of the studies, dofetilide was applied to increase ventricular dispersion in rabbit hearts. This is known to be proarrhythmic, and the introduced heterogeneity in APD across the cardiac wall could be circumvented by application of HERG1 channel activators (Zhou et al., 2005). However, a more thorough examination of the effects of the HERG1 openers in vivo and in intact cardiac tissue has not been described. In a previous report, we examined the in vitro effects of the compound NS1643 (Zhou et al., 2005; Hansen et al., 2006). This compound was difficult to formulate to perform studies on intact tissue, and for this reason, we identified another compound, NS3623, that also increased HERG1 channel activity and in addition can be dissolved in vehicles appropriate for in vivo applications. This article presents a thorough in vitro characterization of NS3623 by experiments conducted after heterologous HERG1 expression in *Xenopus laevis* oocytes and in mammalian human embryonic kidney (HEK) 293 cells. In addition, the ability of NS3623 to affect HERG1 channels under native conditions was investigated using cardiac papillary muscle from guinea pig.

Materials and Methods

Molecular Biology. cDNA encoding either HERG1 (KCNH2, Kv11.1), KCNQ1 (Kv7.1), Kv1.5 (KCNA5), or Kv4.3 (KCND3) channels was introduced into the custom-made vector pXOOM, which is optimized for expression in both *X. laevis* oocytes and mammalian cells (Jespersen et al., 2002). The HERG1 channel mutants HERG1-F656M, HERG1-S620T, and HERG1-S631A were introduced in pSP64. All the HERG1 mutants were a gift from Michael C. Sanguinetti (University of Utah, Salt Lake City, UT).

cRNA preparation and capping were performed by in vitro transcription using the mCAP mRNA capping kit (Stratagene, La Jolla, CA) or Ambion T7 mMessage mMachine kit (Ambion, Austin, TX) according to the manufacturer's instructions. mRNA was phenol/chloroform-extracted, ethanol-precipitated, and dissolved in Tris-EDTA buffer to approximate concentrations of 1 $\mu g/\mu l$. For proof of purity and integrity, mRNA was inspected by gel electrophoresis, and concentrations were determined photometrically. mRNA was stored at −80°C until injection.

Expression in *X. laevis* Oocytes. *X. laevis* surgery and oocyte treatment were done as described previously (Grunnet et al., 2001). Oocytes were collected under anesthesia (Tricain 2 g/l, Sigma A-5040; Sigma-Aldrich, St. Louis, MO) using guidelines approved by the Danish National Committee for Animal Studies. Before injection of 50 nl of mRNA (approximately 50 ng), oocytes were kept for 24 h at 19°C in Kulori medium consisting of 90 mM NaCl, 1 mM KCl, 1 mM $MgCl_2$, 1 mM $CaCl_2$, and 5 mM HEPES, pH 7.4. Injection of mRNA was accomplished using a Nanoject microinjector from Drummond (Drummond Scientific, Broomall, PA). Oocytes were kept at 19°C for 2 to 5 days before measurements were performed.

Expression and Recording in Mammalian Cells. Heterologous expression of HERG1 in mammalian HEK 293 cells and whole-cell patch-clamp recordings were performed as described previously (Hansen et al., 2006).

Isolation of Native Cardiomyocytes. Cells were isolated and incubated as described previously (Hansen et al., 2006).

Native Cardiomyocytes for Recordings of Ca^{2+} and Na^+ Current. Currents were measured with the single electrode voltage-clamp method as described in detail elsewhere (Christ et al., 2005). The pipette solution had the following composition: 90 mM cesium methanesulfonate, 20 mM CsCl, 10 mM HEPES, 4 mM Mg-ATP, 0.4 mM Tris-GTP, 10 mM EGTA, and 3 mM $CaCl_2$, with a calculated free Ca^{2+} concentration of ~60 nM (computer program EQCAL; Bio soft, Cambridge, UK; pH 7.2). Ca^{2+} currents were measured with the following Na^+-free superfusion solution: 120 mM tetraethylammonium chloride, 10 mM CsCl, 10 mM HEPES, 2 mM $CaCl_2$, 1 mM $MgCl_2$, and 20 mM glucose, pH 7.4 (adjusted with CsOH). $I_{Ca,L}$ was measured from a holding potential of −80 mV with test steps (200 ms) between −70 and +65 mV in 5-mV increments at 37°C. For measuring I_{Na}, NaCl (5 mM) was added to the superfusion solution, and $CaCl_2$ was reduced to 0.5 mM. Contaminating $I_{Ca,L}$ was blocked by nisoldipine (1 μM). I_{Na} was measured at room temperature from a holding potential of −100 mV, with test steps (100 ms) between −80 and +5 mV in 5-mV increments. $I_{Ca,L}$ and I_{Na} amplitudes were determined as the difference between peak inward current and current at the end of the depolarizing test step. A system for rapid solution changes allowed application of drugs in the close vicinity of the cells (Cell Micro Controls, Virginia Beach, VA; ALA Scientific Instruments, Long Island, NY).

Papillary Muscle Preparation. Animal handling was performed in accordance with the Helsinki convention. Male Dunkin Hartley Crl: (HA) guinea pigs (Charles River, Sulzfeld, Germany) of 280 to 350 g were sacrificed under light CO anesthesia. Hearts were excised, and thin papillary muscles were removed from the right ventricles. The muscles were mounted in an organ bath continuously perfused with carbogenated Tyrode's solution: 126.7 mM NaCl, 5.4 mM KCl, 1.8 mM $CaCl_2$, 1.05 mM $MgCl_2$, 22 mM $NaHCO_3$, 0.42 mM $NaPO_4$, and 5 mM glucose, pH 7.4, at 37°C. One end of the muscle was pinned to the floor of the chamber, and the free end was connected to a force transducer (AE 801; SensoNor, Dasing, Germany) with silk thread. The muscle was stimulated via Ag/AgCl electrodes at a regular frequency of 1 Hz. After at least 90 min of equilibration, intracellular action potentials were recorded with conventional glass pipettes filled with 2 M KCl (tip resistance 10–20 MΩ). Drugs were added to the superfusion solution. Action potentials from stable impalements were recorded 30 to 45 min after drug addition before the drug concentration was increased. Action potentials were recorded, and the following parameters were analyzed offline: resting membrane potential, action potential amplitude, APD at 20, 50, and 90% of repolarization (APD_{20}, APD_{50}, and APD_{90}), and maximum upstroke velocity (dV/dt_{max}). All the data acquisition and analysis were carried out with the ISO 2 system (MFK, Niedernhausen, Germany).

Analysis of Data. Data analysis and drawings were performed using IGOR software (WaveMetrics, Lake Oswego, OR) or GraphPad Prism software (GraphPad Software, San Diego, CA). All the deviations of calculated mean averages are given as S.E.M. values. EC_{50} values were calculated from equilibrium concentration-response experiments. Data were fitted with a sigmoidal dose-response equation: $Y = \text{Bottom} + (\text{Top-Bottom})/\{1 + 10^{[(\text{LogEC}_{50}-X)\cdot \text{HillSlope}]}\}$, where X is the logarithm of concentration, and Y is the response. Similar activation and inactivation data were fitted with Boltzmann equations. The applied equations were for activation data: $I = I_{max}/\{1 + \exp[(V_{50} - V_t)/k]\}$ and for inactivation data: $I = I_{max}/\{1 + \exp[(V_t -$

$V_{50})/k]\}$, where I is the current, V_{50} is the voltage required for half-activation, V_t is the test membrane potential, and k is the slope factor. To avoid transient capacitance, current values for release from inactivation (Fig. 5) were calculated as the average current amplitude recorded from 10 to 20 ms after the second depolarization step to +20 mV. Time constants for deactivation were calculated by fitting with the double exponential equation $I_{tail} = K_0 + K_{fast} \cdot \exp[-(t/\tau_{fast})] + K_{slow} \cdot \exp[-(t/\tau_{slow})]$, where t is the time in seconds, and the fast and slow deactivation constants are given by τ_{fast} and τ_{slow}, respectively. Finally, the time constant for inactivation was calculated by fitting to the single exponential equation $I_{tail} = K_0 + K \cdot \exp[-(t/\tau)]$, where t is the time in seconds, and τ is the time constant for inactivation. Capacitative current was subtracted before fitting.

Drugs and Solutions. Unless otherwise mentioned, all the chemicals were of analytical grade and were obtained from Sigma. Nisoldipine was a gift of Bayer AG (Wuppertal, Germany). Drugs were dissolved in dimethyl sulfoxide as concentrated stock solutions and diluted directly into the superfusion solution to yield the final concentration. Dimethyl sulfoxide concentration never exceeded 0.1% in final solutions. At this concentration, no influence on any measurements was observed (data not shown).

Results

NS3623 was originally identified as a chloride channel blocker and has shown to be effective in preventing dehydration of erythrocytes (Bennekou et al., 2001). However, this compound also showed an interesting profile when the effect was examined on cloned HERG1 channels; therefore, we chose to examine these effects more thoroughly. Figure 1 presents the structure of NS3623.

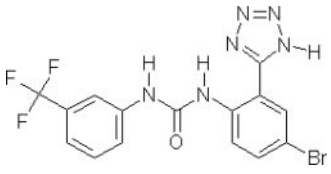

Fig. 1. The structure of NS3623.

The following experiments were designed to obtain detailed information about the effect of NS3623 on cloned HERG1 channels expressed in *X. laevis* oocytes. Figure 2 shows the effect of NS3623 on HERG1-expressing oocytes challenged with the outlined step protocol, where the HERG1 channels were activated by 1-s voltage increments ranging from −80 to +40 mV. These changes in membrane potential evoke a slow voltage-dependent activation of the HERG1 channel followed by strong inactivation, a feature that is reflected in a bell-shaped current-voltage (I-V) relationship (Fig. 2, A and C). The potentials were increased with 10-mV steps, and the tail current was elicited by clamping at −60 mV for 4 s. Summarized I-V relationship for tail currents are shown in Fig. 2D. When a stable control current was obtained, 30 μM NS3623 was added to the bath. In the presence of the compound, both the steady-state and the tail HERG1 currents were increased to a level significantly different from initial control measurements (Fig. 2, B–D). The Boltzmann fits to the activation currents resulted in almost identical V_{50}, where half-maximal activation was −20.0 ± 2 mV in control experiments and −20.0 ± 3 mV in the presence of NS3623. These experiments were repeated with similar results after coexpression of HERG1 and the β-subunit KCNE2 (data not shown). Finally, data were reproduced with HERG1 channels heterologously expressed in mammalian HEK 293 cells (data not shown). To determine the concentration response of NS3623 on heterologously expressed HERG1 channels, oocytes were repeatedly activated by clamping 1 s at

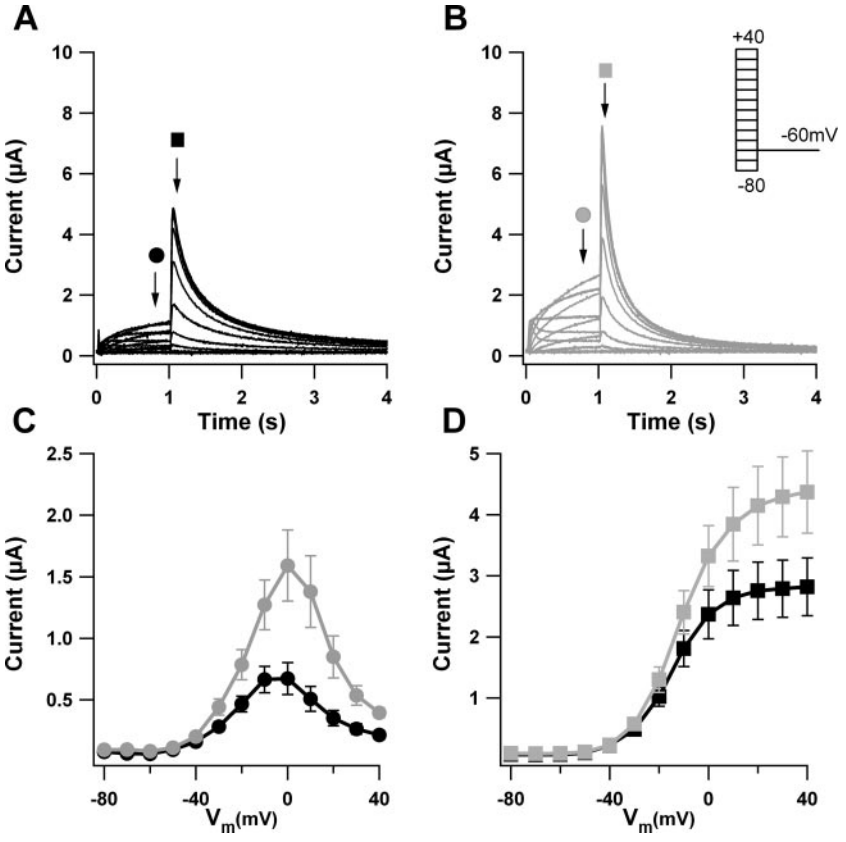

Fig. 2. Activation of the HERG1 channel by 30 μM NS3623. Activating currents elicited by depolarizing voltage in steps of 10 mV in *X. laevis* oocytes injected with HERG1 cRNA in control measurements (A) and after exposure to 30 μM NS3623 (B). C, the characteristic bell-shaped I-V curve of the steady-state curve that is obtained when the oocytes are challenged with the indicated protocol and the corresponding I-V relationship obtained when oocytes were exposed to 30 μM NS3623 (gray). D, the tail currents recorded at −60 mV obtained in control situation (black) and after exposure to NS3623 (gray) (n = 7).

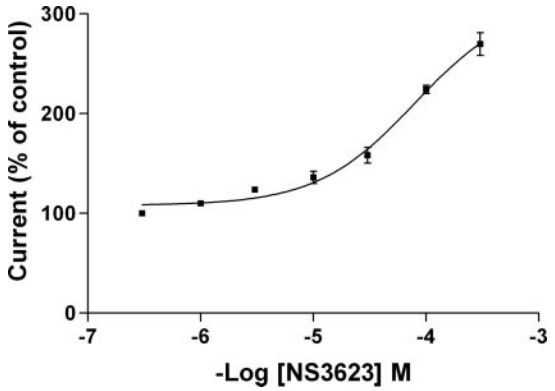

Fig. 3. Concentration response of NS3623 on cloned HERG1 channels. HERG1 channels expressed in *X. laevis* oocytes were repeatedly activated by clamping 1 s at +20 mV, followed by 3 s at −60 mV. Between steps, cells were kept at −80 mV for 3 s. After establishment of stable control current, the oocytes were exposed to increasing doses of NS3623 ranging from 300 nM to 300 μM. Oocytes were washed with Kulori between concentrations. Currents were measured at steady state at +20 mV, normalized to the control current, and plotted as a function of the NS3623 concentration. The dose-effect relationship was sigmoidally fit, and the EC_{50} value was calculated to 79.4 ± 14.9 μM (n = 5).

+20 mV followed by 3 s at −60 mV. Between steps, cells were kept at −80 mV for 3 s. Oocytes were exposed to a series of seven concentrations of NS3623 ranging from 300 nM to 300 μM. Between application of drugs, the oocytes were washed with Kulori solution until a baseline comparable with the initial control values was obtained. The concentration-response relationship with normalized current as a function of drug concentration is depicted in Fig. 3. These currents were sigmoidally fit, and the increase in HERG1 channel activity as a function of concentration was found to have an EC_{50} value of 79.4 ± 14.9 μM.

At the single-channel level, an increase in current from heterologously expressed channels may stem from an increase in the amount of channels expressed or/and an increase in the probability that the ion channel spends a longer time in the open configuration or/and an increase in single channel conductance. An increase in single-channel open probability could result in a number of changes in different kinetic parameters that each could contribute to augment the total HERG1 current. The increase in overall HERG1 channel conductance may for example be caused by a slowing of

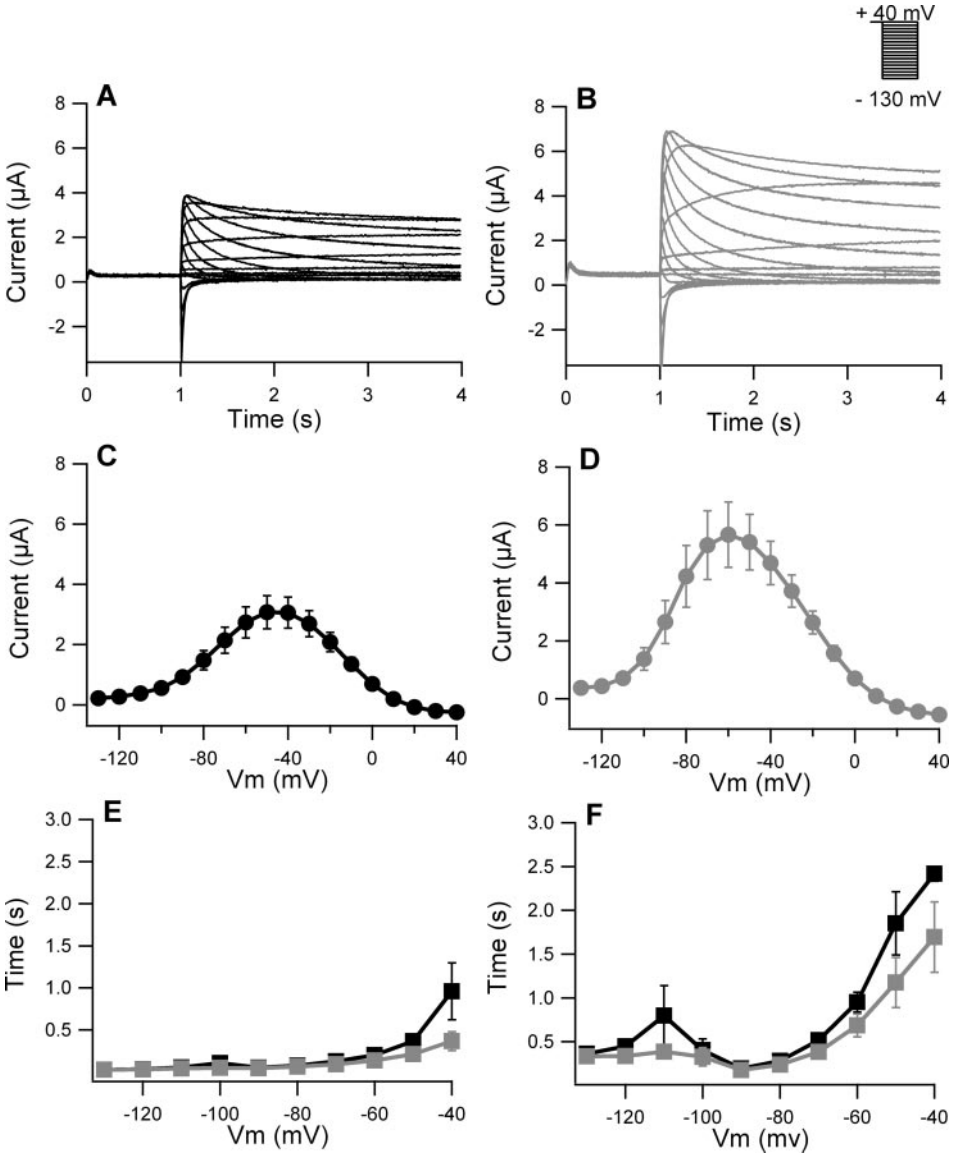

Fig. 4. NS3623 does not affect deactivation of the HERG1 channel. The voltage dependence and time constants of channel deactivation were investigated using the outlined protocol, where current was activated with a 1-s pulse at +40 mV, followed by a 10-mV stepped test potential ranging from −130 to +40 mV to determine the voltage dependence of deactivation in control oocytes (A) and after exposure to 30 μM NS3623 (B). The peak tail current as a function of the applied voltage used to release the channels from inactivation is depicted in C. In the presence of 30 μM NS3623, the tail current increased at most potentials (D). Time constants for deactivation were calculated from two exponential fits to the recorded tail currents. Neither the fast (E) nor the slow (F) component changed significantly when the channels were exposed to NS3623 (n = 6).

the deactivation time constants. To test this hypothesis, oocytes expressing HERG1 channels were subjected to a voltage-clamping protocol where channels first were fully activated and inactivated by a clamp of +40 mV for 1 s, followed by steps from −130 to +40 mV lasting for 4 s in steps of 10 mV to reveal the deactivation kinetic. Oocytes were clamped for 3 s at −80 mV between the steps, and the resulting tail currents were measured. Representative current traces for control current are depicted in Fig. 4A, and summarized I-V relationship is shown in Fig. 4C. In the presence of 30 μM NS3623, the peak tail current increased relative to the control experiments as can be seen from representative current traces in Fig. 4B. In addition, the voltage that elicited the largest current was changed from −50 to −60 mV as can be seen from the I-V relationship presented in Fig. 4, C (control) and D (NS3623). Deactivating tail currents were fitted with a two exponential function revealing the time constants for both fast and slow deactivation (Fig. 4, E and F). NS3623 (30 μM) did not induce a significant change in either the slow or fast time constants for deactivation. We then investigated the ability of NS3623 to change the response to voltage-dependent release from inactivation on HERG1 channels (Fig. 5). Oocytes were exposed to a tripulse protocol, where the channels were completely activated and inactivated by holding the membrane potential at +20 mV for 1 s, followed by very short (10 ms) repolarizing steps from −150 to +20 mV, and finally clamping again at +20 mV for 1 s. Application of this protocol makes it possible to reveal how release of inactivation is affected by the preceding voltage. This information is obtained by plotting the peak current resulting from the last step to +20 mV as a function of the previous short-step potential. The normalized data were fitted with a Boltzmann function. In the control oocytes, V_{50} was −75.9 ± 0.6 mV, and for oocytes exposed to 30 μM NS3623 V_{50} was calculated to −58.2 ± 0.4 mV (n = 6) (Fig. 5C). This rightward shift of 17.7 mV in V_{50} may explain the increase in current through HERG1 channels exposed to NS3623.

To further investigate how NS3623 could affect the inactivation properties of HERG1 channels, a protocol designed to examine the time course of the inactivation was applied. This protocol was initially described by Smith et al. (1996) and Spector et al. (1996) and is outlined in Fig. 6. Channels were first activated and then inactivated by a 1-s pulse to +40 mV. Thereafter, the channels were subjected to a 10-ms pulse at −120 mV to allow full recovery from inactivation. The 10-ms time span at −120 mV is at the same time sufficiently short to prevent the channels from initiating deactivation. The third part of this pulse was a stepwise increment in the potential from −40 to +50 mV lasting for 1 s, to elicit a re-onset of channel inactivation. The currents representing this re-onset of inactivation were then fitted with a monoexponential function. When comparing the resulting time constants from NS3623-treated oocytes with control experiments, it was revealed that time constants were significantly and immensely increased at all the measured potentials in the presence of 30 μM NS3623 (Fig. 6).

Having addressed the ability of NS3623 to affect activation, deactivation, and inactivation of HERG1 channels, the mode of action of NS3623 was further investigated by application of different HERG1 channel mutants. To test whether NS3623 could activate HERG1 channels not capable of inactivation, the effect of the compound was investigated on

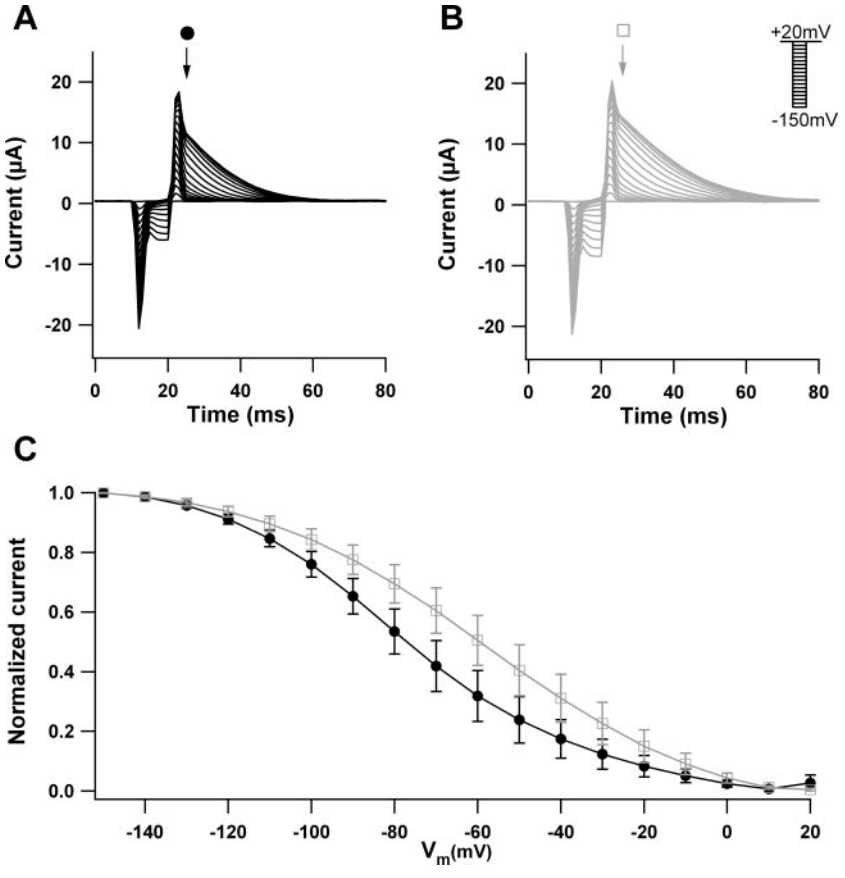

Fig. 5. NS3623 influences the half-point of voltage-dependent inactivation. Channels were completely activated and inactivated by holding the membrane potential at +20 mV for 1 s followed by very short (10-ms) repolarizing steps from −150 to 20 mV and, finally, clamping at 20 mV. Representative data for control oocytes (black) and oocytes exposed to 30 μM NS3623 (gray) are shown in A and B, respectively. The peak tail current was then recorded and plotted as a function of the previous short-step potential, which makes it possible to investigate the voltage dependence of release from inactivation (C). The normalized data for control oocytes (black) and oocytes exposed to 30 μM NS3623 (gray) were fitted to a Boltzmann function. In control oocytes, V_{50} was −75.9 ± 0.6 mV, and for oocytes exposed to 30 μM NS3623, V_{50} was calculated to −58.2 ± 0.4 mV (n = 6).

channels that do not (HERG1 S620T) or only to a small degree (HERG1 S631A) inactivate (Zou et al., 1998, Casis et al., 2006). The step protocol described in Fig. 2 was used to elicit the mutant HERG1 current, and 30 μM NS3623 was applied when stable control currents were obtained. The activity of the HERG1 S620T mutant in the absence (Fig. 7A) or presence (Fig. 7B) of 30 μM NS3623 was investigated. The steady-state I-V relationship summarized in Fig. 7C revealed no significant difference in oocytes treated with the drug compared with the controls. Similar results were obtained with the S631A mutant that only has a very small degree of inactivation in the absence (Fig. 7D) or presence (Fig. 7E) of 30 μM NS3623. Summarized data are depicted in Fig. 7F. Although no significant difference was observed in the I-V relationship of the drug-induced response compared with controls, there was tendency toward larger steady-state currents in the presence of NS3623. Having established that the ability of NS3623 to increase HERG1 current is severely reduced in noninactivating channels, the mode of action of NS3623 was further explored using HERG1 channels mutated in the high-affinity pore blocker residue F656. Mutating this residue from phenylalanine to methionine (F656M) greatly reduces the affinity of a number of HERG1 channel inhibitors (Lees-Miller et al., 2000; Mitcheson et al., 2005). Interestingly, when the 30 μM NS3623 was examined on the mutated channel HERG1 F656M, a very large increase in the current response (approximately 5 times) was observed as can be seen in Fig. 8. This indicates that NS3623 also is acting as a partial blocker of the HERG1 channels. As a final biophysical characterization of NS3623, it was investigated whether the compound could activate closed HERG1 channels. Continuous opening and closing of HERG1 channels

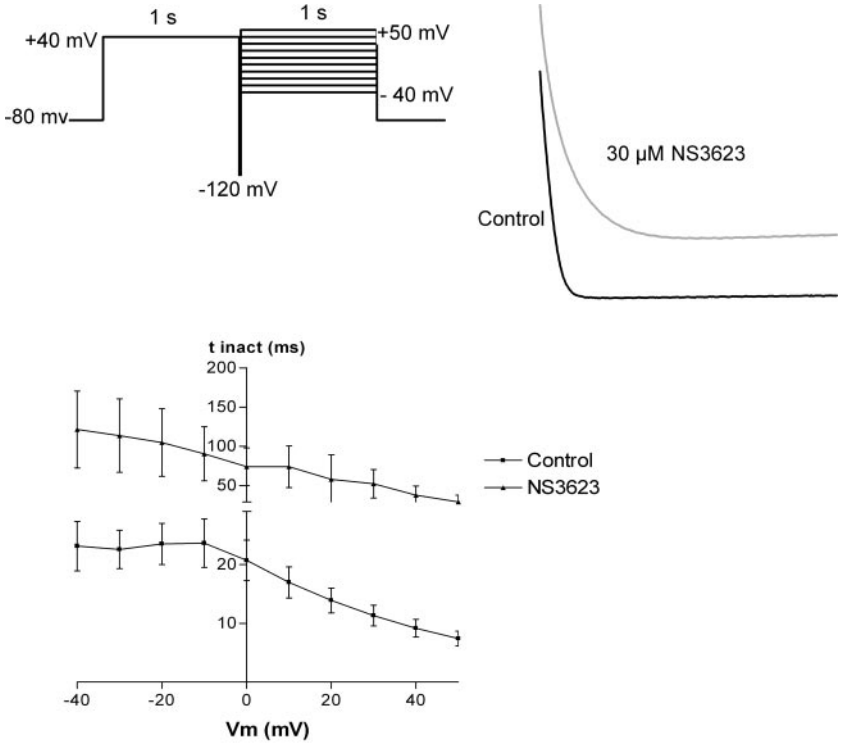

Fig. 6. The time constant for re-onset of inactivation is affected by NS3623. Current was first activated and then inactivated by a 1-s pulse to 40 mV. Thereafter, the channels were subjected to a 10-ms pulse to allow complete recovery from inactivation. The third part of the outlined pulse was a stepwise increment in the potential from −40 to +50 mV to elicit a re-onset of channel inactivation. The currents representing the re-onset of inactivation were then fitted to a monoexponential function. When comparing the resulting time constants from NS3623-treated oocytes with control experiments, it was revealed that these constants were significantly and immensely increased at all the measured potentials (n = 4).

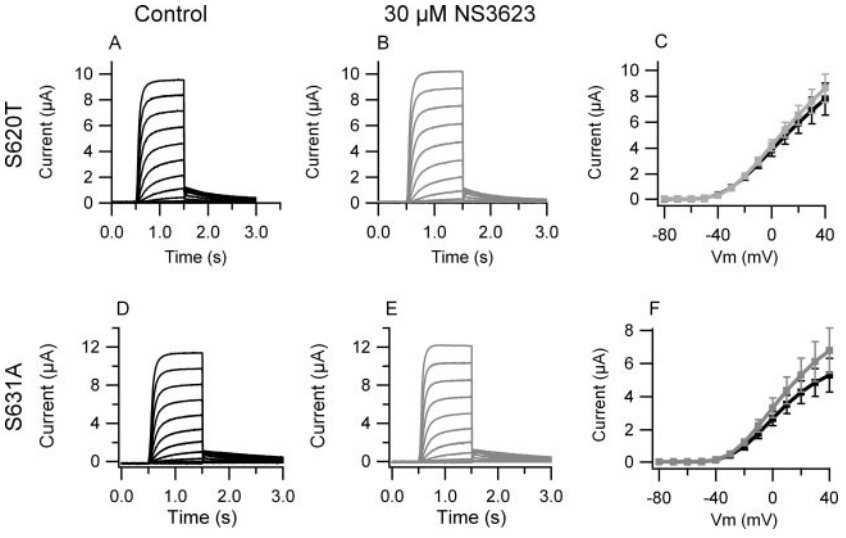

Fig. 7. No effect of NS3623 on noninactivating mutants. To test whether NS3623 could increase activity of HERG1 channels not capable of inactivation, the effect of the compound was investigated on channels that do not (S620T) or only to a small extent (S631A) inactivate. The step protocol outlined in Fig. 2 was used to elicit the mutant HERG1 current, and 30 μM NS3623 was applied when stable control currents were obtained. Control recordings of S620T are shown in black in A, and recordings in the presence of 30 μM NS3623 are shown in gray in B. The summarized steady-state I-V relationship depicted in C reveals no significant difference in oocytes treated with NS3623 compared with the controls. Similar results were obtained with the S631A mutant that only has a very small degree of inactivation (D–F) (n = 4).

were obtained by a repeated two-step protocol with 200 ms at +20 mV, followed by 800 ms at −80 mV. NS3623 (30 μM) was applied, and the time scale for complete compound effect was determined (Fig. 9A). Compound application was also performed to channels where the repeated step protocol was interrupted by a continuous clamp at −80 mV to keep the

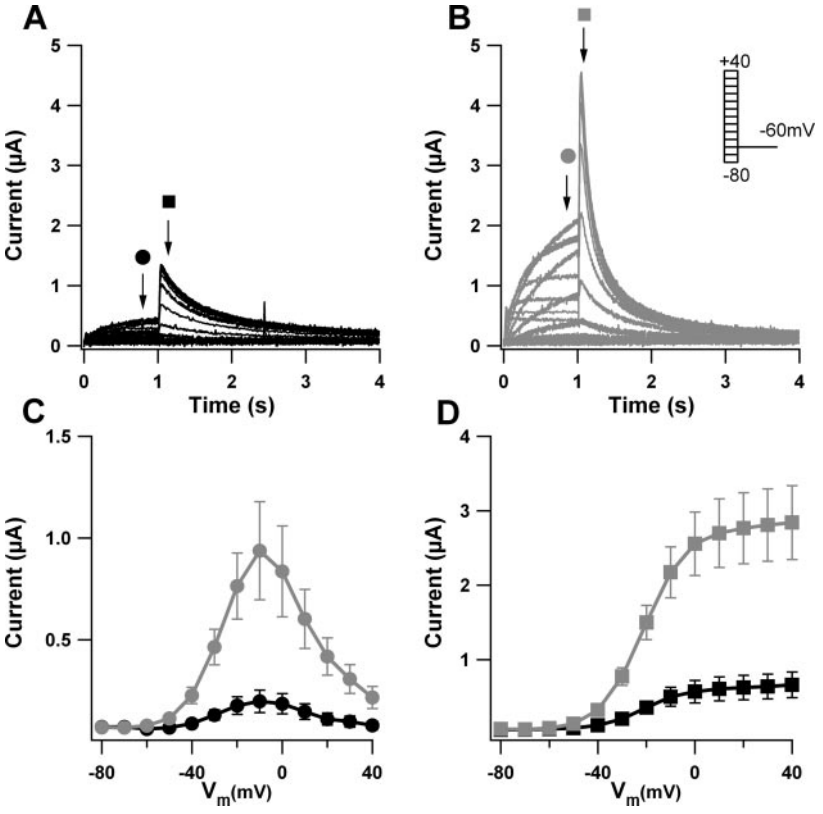

Fig. 8. Increased potency of NS3623 on mutant with altered blocking site. F656M HERG1 channels expressed in oocytes were challenged with the protocol described in Fig. 2. A and B, representative traces of results obtained from control oocytes and from oocytes exposed to NS3623, respectively. Both steady-state (C) and tail currents (D) were increased approximately 5 times in the presence of NS3623 (gray traces) (n = 5).

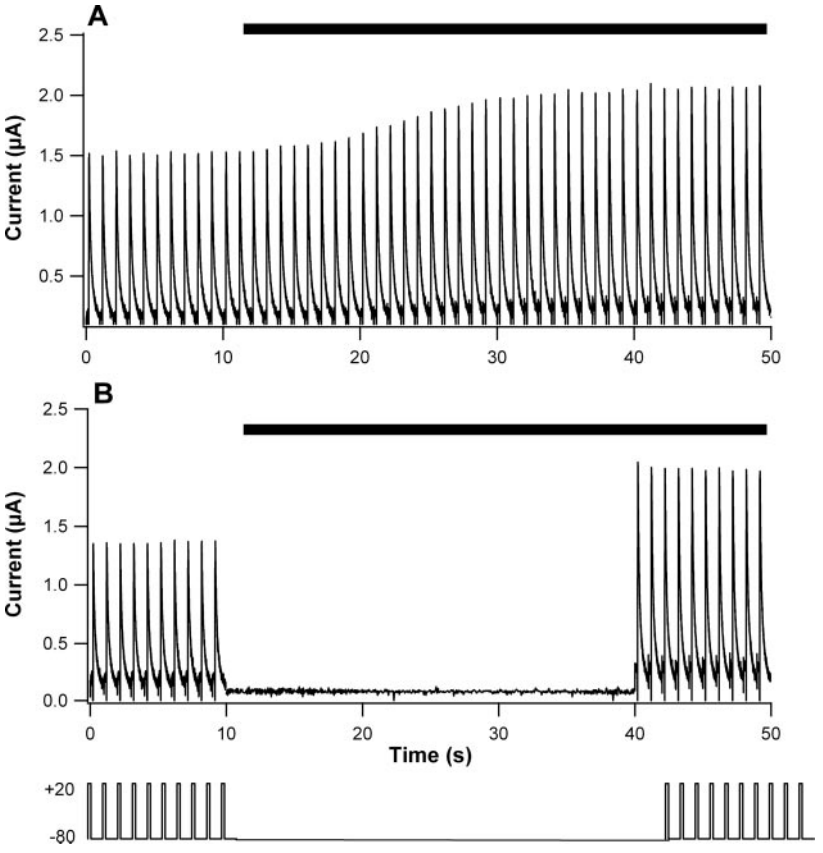

Fig. 9. NS3623 can bind to closed HERG1 channels. HERG1 channels were continuously opened and closed by a repeated two-step protocol with 200 ms at +20 mV followed by 800 ms at −80 mV. Black bars indicate application 30 μM NS3623. The time scale for full compound effect was determined (A). Compound application was also performed to channels where the repeated step protocol was interrupted by a continuous clamp at −80 mV to keep the channels closed (B). After resuming the repeated step protocol, an instant current increase to 144 ± 14% was observed (n = 4).

channels closed. After resuming the repeated step protocol, an instant current increase to 144 ± 14% was observed, indicating that NS3623 can bind to closed channels ($n = 4$).

To test the ability of NS3623 to act as an antiarrhythmic compound, HERG1 channel activity was monitored during a cardiac action potential stimulus. The action potential-like protocol is shown in Fig. 10. Application of the outlined protocol resulted in a gradual increase of the steady-state current during the "plateau phase" of the action potential, which reached a maximum during the end of this depolarized phase, and a tail current was elicited on repolarization. When the oocytes were exposed to 30 μM NS3623, both the steady-state and the tail current increased, but no change in the gradual onset of the steady-state current was observed.

The selectivity of NS3623 for HERG1 over other important cardiac potassium ion channels was examined, and representative traces are presented in Fig. 11. Measurements were performed from oocytes expressing either KCNQ1 (Fig. 11A), Kv1.5 (Fig. 11B), or Kv4.3 channels (Fig. 11C). KCNQ1 participates in cardiac I_{Ks} current, Kv1.5 in I_{Kur} current, and Kv4.3 in I_{to} current. The protocols outlined in the figure legend were used to elicit the respective currents. KCNQ1, Kv1.5, and Kv4.3 channels were unaffected by the presence of 30 μM NS3623. We then further examined the effect of NS3623 on native calcium and sodium currents measured from isolated guinea pig cardiomyocytes. The results obtained for 10 μM of the compound are shown in Fig. 12, A and B (calcium current) and C and D (sodium current). Effect of NS3623 on inward currents I_{Ca} in guinea pig ventricular myocytes showed a substantial and variable run-down over time. Five minutes after establishing access, the cells were exposed to 10 μM NS3623. $I_{Ca,L}$ density was 20.1 ± 3.4 pA/pF before and 19.1 ± 3.7 pA/pF after drug exposure ($n = 7$). This decline was not different compared with spontaneous run-down in time-matched controls (data not shown). NS3623 also did not affect $I_{Ca,T}$ (Fig. 12A). However, a small block of 20% of the L-type calcium currents was observed in the presence of 30 μM of the compound, whereas 100 μM inhibited the current by 40%. I_{Na} was stable over time, and I_{Na} density 2 min after exposure to NS3623 was not different from the control values (46.5 ± 7.3 versus 46.8 ± 7.5 pA/pF, $n = 5$). The small Na^+ current was unaffected by 30 and 100 μM NS3623 (data not shown). We then examined the effect of activating HERG1 channels by NS3623 in isolated papillary muscle (Fig. 13). Under control conditions, APD_{20}, APD_{50}, and APD_{90} were 80 ± 3, 133 ± 4, and 154 ± 5 ms, respectively ($n = 5$), and remained stable in time-matched control experiments. Exposure to 10 μM NS3623 decreased APD_{20}, APD_{50}, and APD_{90} to 67 ± 3, 112 ± 6, and 131 ± 8 ms, respectively ($p < 0.05$). Moreover, NS3623 (10 μM) reduced force of contraction when compared with the time-matched control (from 122 ± 45 to 53 ± 23 μN in NS3623 versus from 118 ± 12 to 78 ± 10 μN in TMC, $n = 5$ each group). Resting membrane potential, dV/dt_{max}, and action potential amplitude were not affected by NS3623. Control values were −87 ± 0.5 mV, 238 ± 13 V/s, and 125 ± 1 mV, respectively ($n = 5$).

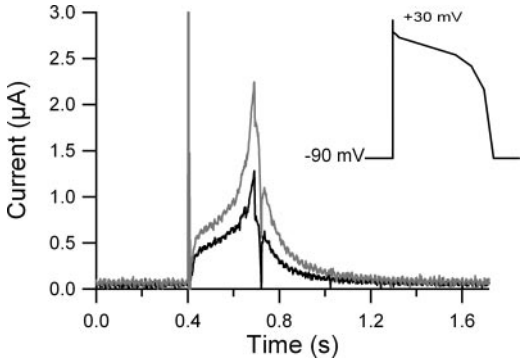

Fig. 10. Maintenance of normal action potential shape of the HERG1 current on exposure to NS3623. HERG1 currents were elicited with stimuli imitating cardiac ventricular action potentials. The black trace is representative of currents obtained in control situations with a gradual increase of the steady-state current during the "plateau" phase of the action potential that reaches maximum at the end of this depolarized phase and a smaller tail current that is elicited on repolarization. When the oocytes were exposed to 30 μM NS3623, both the steady-state and the tail current were increased, but no change in the gradual onset of the steady state was observed (gray trace) ($n = 5$).

Discussion

Very recently, we have shown that the diphenylurea NS1643 is an activator of HERG1 potassium channels (Hansen et al., 2006). It has so far been impossible to obtain a formulation of NS1643 for in vivo purposes. Because we

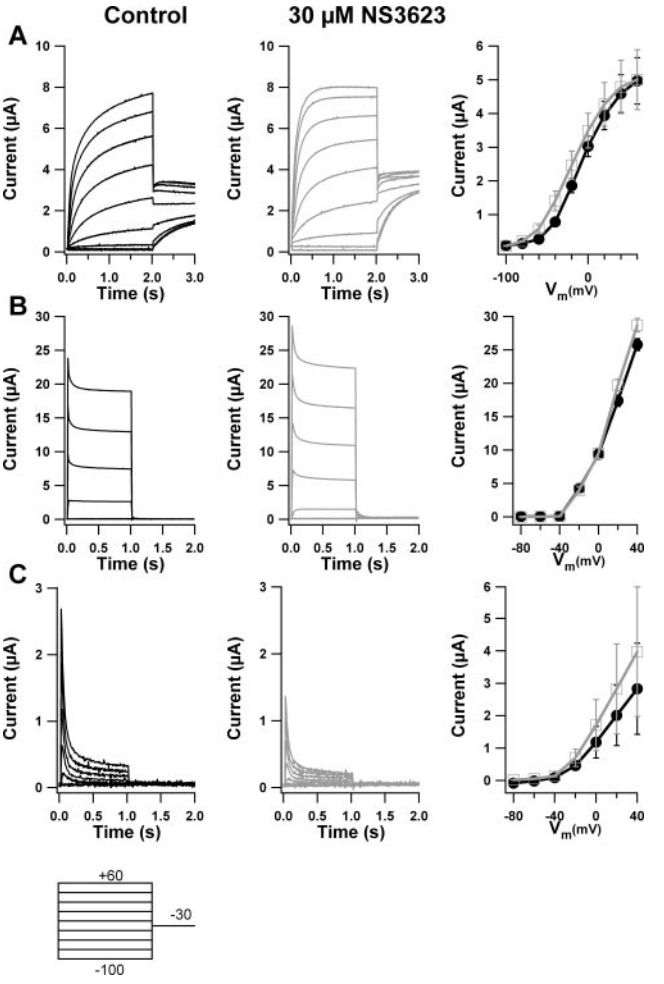

Fig. 11. NS3623 is not affecting other important cardiac potassium channels. The selectivity of NS3623 for HERG1 over other potassium channels was examined, and representative traces are presented for KCNQ1 (A), Kv1.5 (B), and Kv4.3 (C) channels. The protocols outlined next to the traces were used to elicit the respective currents. None of the investigated channels were significantly affected by the presence of 30 μM NS3623 ($n = 3$).

strongly believe there is a need for HERG1-activating compounds that can be used in experiments using isolated cardiac tissue and for in vivo applications, we searched for another compound that had the ability of activating the HERG1 channel. The present experiments were performed to examine the in vitro effects of the compound NS3623. In contrast to NS1643, this compound can be dissolved in vehicles appropriate for in vivo experiments. Initially, NS3623 has been tested in vivo and identified as a chloride channel blocker with the availability to inhibit the dehydration of red blood cells that occurs in sickle cell disease (Bennekou et al., 2001). It cannot be completely ruled out that any observed effect of NS3623 in the present and future assays is to some extent mediated by a block of chloride channels. However, although it has been reported that $I_{Cl,vol}$ is present in the mammalian myocardium (Zou et al., 1998; Decher et al., 2001), a block of this current is not expected to influence the duration of the action potential in normal cardiac tissue.

Until very recently, no activators of the HERG1 channel have been known, and understanding how compounds can increase the current through this important cardiac channel is crucial because it can be speculated that such a drug is beneficial in the treatment of certain kinds of arrhythmias. An overall increase of HERG1 channel current may stem from an increase in channel protein insertion in the cell membrane, and/or an increase in the open probability of the channel, and/or a change in single-channel conductance. In the present experiments, the increase of current was immediate as the drug was added to the perfusion solution, which makes it highly unlikely that NS3623 induces a higher expression of HERG1 channel in the oocyte. NS3623 was found to predominantly increase HERG1 current by affecting channel inactivation. When investigating the voltage-dependent release from inactivation, we observed a rightward shift of 17.7 mV of the half-inactivation voltage; i.e., channels will more easily be released from inactivation at any given membrane potential during repolarization and at the resting membrane potential in the cardiac diastole. Therefore, it follows that in the presence of NS3623 more channels are expected to be available at physiological relevant potentials compared with controls (Fig. 5C). We also found that the onset of inactivation was dramatically slowed at all the measured potentials (Fig. 6B). The profound influence of NS3623 on the inactivation kinetics of the HERG1 channel may fully account for the observed increase in current. Because inactivation holds channels in a nonconducting conformation, rightward shifting the voltage at which half of the channels are inactive makes more channels available at most physiologically relevant membrane potentials. Therefore, it can be hypothesized that during the action potential, exposure of the cardiomyocyte to NS3623 will increase the repolarizing reserve.

We also investigated the effect of NS3623 on channel activation, and although there was an overall increase in the steady-state and tail current in the drug-treated oocytes, we found no significant difference in the voltage dependence of activation (Fig. 2). When deactivation time course was investigated, we did not find any significant changes in the presence of NS3623 compared with control (Fig. 4). However, NS3623 induced a shift in the voltage that induced the largest tail current (Fig. 4, C and D). Under control conditions, the largest current was induced at −50 mV, whereas application of NS3623 resulted in a 10-mV shift toward a more negative potential. Such a shift may be speculated to increase the repolarizing reserve and the diastolic HERG1 current of cardiac myocytes exposed to drugs like NS3623 because the larger tail current will appear later in the repolarizing phase of the action potential.

In mutant channels where the inactivation ability was compromised (HERG1 S620T and HERG1 S631A) or where the blocking site was eliminated (HERG1 F656M), the mechanism of action of NS3623 was further revealed. When the compound was examined by application to the noninactivating HERG1 mutant S620T, no significant increase in current was observed (Fig. 7C). Neither did NS3623 significantly increase currents measured from the S631A mutated chan-

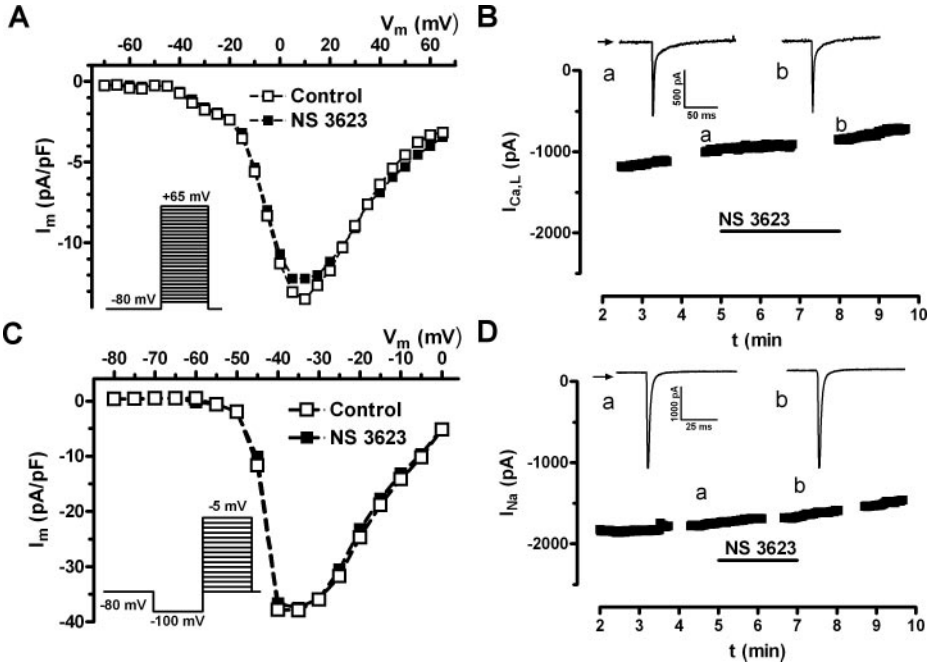

Fig. 12. Effect of NS 3623 on I_{Ca} and I_{Na} in guinea pig ventricular myocytes. Current-voltage relationship for Ca^{2+} current recorded before and 2 min after the addition of 10 μM NS 3623 (A). The small shoulder in the I-V curve between −45 and −20 mV represents T-type Ca^{2+} current; the remaining current (peak at +5 mV) is caused by L-type current. Time course of peak $I_{Ca,L}$ (B). Current-voltage relationship for I_{Na} (C). Time course for peak I_{Na} (D). Insets in A and C, voltage protocols; in B and D, original traces obtained at times marked by "a" and "b", respectively. The horizontal bars indicate the time of drug exposure.

nel (Fig. 7C), a channel that has been reported to possess a slight inactivation (Zou et al., 1998). This is consistent with the finding that NS3623 most dominantly affects the rapid C-type inactivation that occurs during normal HERG1 channel activation. Addition of NS3623 to channels mutated in one of two amino acids necessary for high-affinity HERG1 channel inhibition (F565M) resulted in a ~5-fold increase of the steady-state current at 0 mV and a ~5-fold increase in the tail current likewise measured at 0 mV (Fig. 8). When these data are compared with results obtained after NS3623 application to wild-type HERG1 channels (Fig. 2), it is obvious that NS3623 is a far more potent HERG1 channel activator when part of the high-affinity HERG1 channel inhibitor site is mutated. Therefore, it can be concluded that NS3623 must have a dual mode of action with a combined inhibitory and activating function. It should be emphasized that the overall mode of action of NS3623 is to increase wild-type HERG1 current, showing that the activating function of NS3623 is superior to the inhibitory activity of the compound. Finally, it was shown that NS3623 can bind to and activate closed HERG1 channels. This indicates that the binding site for NS3623 may be at the extracellular part of the channel.

Recently, attention has been drawn to the short QT syndrome, where an apparent gain-of function mutation of the HERG1 channels gives rise to lethal cardiac arrhythmias. Gussak et al. (2000) first described that short QT intervals on the electrocardiogram increase the risk of sudden cardiac death to the same extent as the long QT, and it can be speculated whether drugs that increase the HERG1 current and thereby decrease the APD will be proarrhythmic. It has been shown that the short LQT1 syndrome is caused by a gain-of-function mutation in the HERG1 channel by an N588K (asparagine to lysine) mutation that is located in the S5-pore linker region and gives rise to a HERG1 current with a large steady-state current but a very small tail current (Zou et al., 1998; Brugada et al., 2004; Cordeiro et al., 2005; McPate et al., 2005). The small tail current will result in less repolarization reserve in the myocardium. Therefore, it can be argued that even though HERG1 N588K is reported as a gain-of-function in the steady-state current, it can equally well be revealed as a loss of function when it comes to participation in cardiac action potential repolarization. Moreover, this mutation affects the recovery of inactivation, extensively resulting in an almost 100-mV rightward shift in the voltage-dependence HERG1 channel availability. We observed a rightward shift of 17 mV, which means that NS3623 induces a shift in the potential where half of the channels will be inactivated toward more depolarized potentials, resulting in a larger steady-state current. However, HERG1 channels exposed to NS3623 will still be expected to inactivate during the plateau phase of the action potential, considering the moderate shift in the estimated half-point of mid-inactivation. Furthermore, McPate et al. (2005) and Cordeiro et al. (2005) reported that the N588K mutation resulted in a HERG1 current that monotonously followed the action potential wave form when such a protocol was applied, which is in contrast to the wild-type HERG1 current where the steady state reaches a peak current during the plateau phase. When we applied an action potential wave form to elicit HERG1 current, we observed that the shape of the current did not change when the oocytes were exposed to NS3623, although the current did increase in magnitude as seen on Fig. 10. Therefore, it is highly likely that HERG1 channel activation by NS3623 is incomparable with the HERG1 N588K gain-of-function mutation.

In the isolated papillary muscle from guinea pigs, we observed a shortening of the action potential (Fig. 13). In the presence of 10 μM NS3623, APD_{90}, APD_{50}, and APD_{20} decreased to the same extent, indicating a uniform abbreviation of repolarization. In the studies of selectivity for NS3623 for HERG1 channels over other relevant cardiac channels, we did not observe any significant changes in the native sodium and calcium currents (Fig. 12), a finding that is consistent with the maintenance of "normal" action potential appearance. Neither did NS3623 significantly affect KCNQ1, Kv1.5, or Kv4.3, indicating that the abbreviation of the APD is mainly through activation of the HERG1 channel.

We conclude that NS3623 can be seen as a selective HERG1 channel opener when applied in cardiac tissue. Furthermore, NS3623 activation of HERG1 channels is fundamentally different from currents recorded from gain-of-function HERG1 N588K mutations. Having the good solubility profile of NS3623 in mind, we therefore believe that a proper tool compound has been obtained to address questions regarding HERG1 opening in intact tissue and after in vivo applications. These approaches will be addressed in future studies.

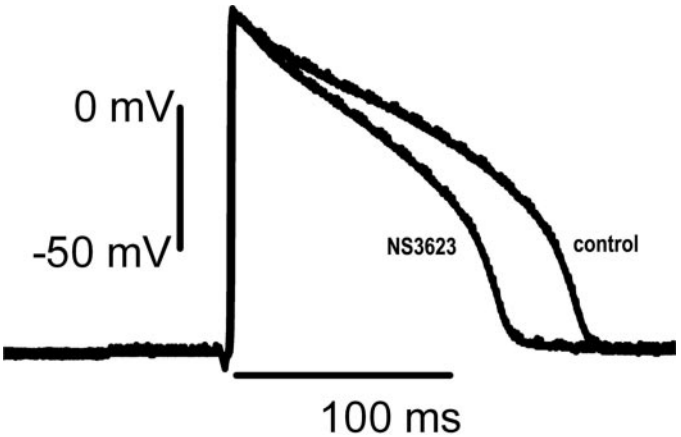

Fig. 13. Papillary muscle. Effect of NS3623 on action potentials recorded in papillary muscle. Application of 10 μM NS3623 to isolated papillary muscle caused a significant shortening of APD at 20, 50, and 90% of repolarization (APD_{20}, APD_{50}, and APD_{90}) relative to the stable control recordings. The resting membrane potential and the upstroke velocity were not affected during drug application.

Acknowledgments

We thank Camilla Irlind for excellent technical assistance.

References

Barhanin J, Lesage F, Guillemare E, Fink M, Lazdunski M, and Romey G (1996) K(V)LQT1 and LsK (MinK) proteins associate to form the I(Ks) cardiac potassium current. *Nature (Lond)* **384:**78–80.

Bennekou P, de Franceschi L, Pedersen O, Lian L, Asakura T, Evans G, Brugnara C, and Christophersen P (2001) Treatment with NS3623, a novel Cl-conductance blocker, ameliorates erythrocyte dehydration in transgenic SAD mice: a possible new therapeutic approach for sickle cell disease. *Blood* **97:**1451–1457.

Brugada R, Hong K, Dumaine R, Cordeiro J, Gaita F, Borggrefe M, Menendez TM, Brugada J, Pollevick GD, Wolpert C, et al. (2004) Sudden death associated with short-QT syndrome linked to mutations in HERG. *Circulation* **109:**30–35.

Casis O, Olesen SP, and Sanguinetti MC (2006) Mechanism of action of a novel human ether-a-go-go-related gene channel activator. *Mol Pharmacol* **69:**658–665.

Christ T, Wettwer E, and Ravens U (2005) Risperidone-induced action potential

prolongation is attenuated by increased repolarization reserve due to concomitant block of I(Ca,L). *Naunyn-Schmiedeberg's Arch Pharmacol* **371:**393–400.
Cordeiro JM, Brugada R, Wu YS, Hong K, and Dumaine R (2005) Modulation of I(Kr) inactivation by mutation N588K in KCNH2: a link to arrhythmogenesis in short QT syndrome. *Cardiovasc Res* **67:**498–509.
Decher N, Lang HJ, Nilius B, Bruggemann A, Busch AE, and Steinmeyer K (2001) DCPIB is a novel selective blocker of I(CL,Swell) and prevents swelling-induced shortening of guinea-pig atrial action potential duration. *Br J Pharmacol* **134:** 1467–1479.
Fitzgerald PT and Ackerman MJ (2005) Drug-induced torsades de pointes: the evolving role of pharmacogenetics. *Heart Rhythm* **2:**S30–S37.
Grunnet M, Jensen BS, Olesen SP, and Klaerke DA (2001) Apamin interacts with all subtypes of cloned small-conductance Ca^{2+}-activated K+ channels. *Pflueg Arch Eur J Physiol* **441:**544–550.
Gussak I, Brugada J, Wright RS, Kopecky SL, Chaitman BR, and Bjerregaard P (2000) Idiopathic short QT interval: a new clinical syndrome? *Cardiology* **94:**99–102.
Hansen RS, Diness TG, Christ T, Demnitz J, Ravens U, Olesen SP, and Grunnet M (2006) Activation of human ether-a-go-go-related gene potassium channels by the diphenylurea 1,3-bis-(2-hydroxy-5-trifluoromethyl-phenyl)-urea (NS1643). *Mol Pharmacol* **69:**266–277.
Jespersen T, Grunnet M, Angelo K, Klaerke DA, and Olesen SP (2002) Dual-function vector for protein expression in both mammalian cells and Xenopus laevis oocytes. *Biotechniques* **32:**536–540.
Kang J, Chen XL, Wang H, Ji J, Cheng H, Incardona J, Reynolds W, Viviani F, Tabart M, and Rampe D (2005) Discovery of a small molecule activator of the human ether-a-go-go-related gene (HERG) cardiac K+ channel. *Mol Pharmacol* **67:**827–836.
Lees-Miller JP, Duan Y, Teng GQ, and Duff HJ (2000) Molecular determinant of high-affinity dofetilide binding to HERG1 expressed in Xenopus oocytes: involvement of S6 sites. *Mol Pharmacol* **57:**367–374.
McPate MJ, Duncan RS, Milnes JT, Witchel HJ, and Hancox JC (2005) The N588K-HERG K+ channel mutation in the 'short QT syndrome': mechanism of gain-in-function determined at 37 degrees C. *Biochem Biophys Res Commun* **334:**441–449.
Mitcheson J, Perry M, Stansfeld P, Sanguinetti MC, Witchel H, and Hancox J (2005) Structural determinants for high-affinity block of HERG potassium channels. *Novartis Found Symp* **266:**136–150.
Sanguinetti MC, Curran ME, Zou A, Shen J, Spector PS, Atkinson DL, and Keating MT (1996) Coassembly of K(V)LQT1 and MinK (IsK) proteins to form cardiac I(Ks) potassium channel. *Nature (Lond)* **384:**80–83.
Sanguinetti MC, Jiang C, Curran ME, and Keating MT (1995) A mechanistic link between an inherited and an acquired cardiac arrhythmia: HERG encodes the IKr potassium channel. *Cell* **81:**299–307.
Smith PL, Baukrowitz T, and Yellen G (1996). The inward rectification mechanism of the HERG cardiac potassium channel. *Nature* (*Lond*) **379:**767–768.
Spector PS, Curran ME, Zou A, Keating MT, and Sanguinetti MC (1996) Fast inactivation causes rectification of the IKr channel. *J Gen Physiol* **107:**611–619.
Trudeau MC, Warmke JW, Ganetzky B, and Robertson GA (1995) HERG, a human inward rectifier in the voltage-gated potassium channel family. *Science (Wash DC)* **269:**92–95.
Zhou J, Augelli-Szafran CE, Bradley JA, Chen Y, Koci BJ, Volberg WA, Sun Z, and Cordes JS (2005) Novel potent human ether-a-go-go-related gene (hERG) potassium channel enhancers and their in vitro antiarrhythmic activity. *Mol Pharmacol* **68:**876–884.
Zou A, Xu QP, and Sanguinetti MC (1998) A mutation in the pore region of HERG K+ channels expressed in Xenopus oocytes reduces rectification by shifting the voltage dependence of inactivation. *J Physiol* **509 (Pt 1):**129–137.

Address correspondence to: Morten Grunnet, NeuroSearch A/S, Pederstrupvej 93, DK-2750 Ballerup, Denmark. E-mail: mgr@neurosearch.dk